Tikrit Journal of Engineering Sciences (2025); 32(3): 1548
DOI: http://doi.org/10.25130/tjes.32.3.1

IRAQI Academic Scientific Journals

ISSN: 1813-162X (Print); 2312-7589 (Online)

Tikrit Journal of Engineering Sciences

available online at: http://www.tj-es.com

TJES Tikrit Journal of Engineering Sciences

Wind Disturbance Rejection of a Foldable Quadrotor Using Nonlinear PID-based Sliding Mode Control

Reyam G. Ghane *, Mohammed Y. Hassan

Control and Systems Engineering Department, University of Technology, Baghdad, Iraq.

Keywords:

Foldable quadrotor; Sliding mode control; Nonlinear PID; Wind gust.

Highlights:

- *Dual-loop control (nonlinear PID + sliding mode) ensures 98% trajectory accuracy under wind gusts.*
- *Foldable quadrotor adapts morphology with 1 m/s wind resistance via robust controllers.*
- *Simulations show minimal overshoot (7.5×10^{-3}) and undershoot (6.7×10^{-2}) during wind disturbances.*
- *MATLAB/Simulink validates stability during shape-shifting and turbulence.*

ARTICLE INFO

Article history:

Received	14 Aug.	2023
Received in revised form	03 Dec.	2023
Accepted	28 July	2024
Final Proofreading	07 Oct.	2024
Available online	17 June	2025

Citation: Ghane RG, Hassan MY. **Wind Disturbance Rejection of a Foldable Quadrotor Using Nonlinear PID-based Sliding Mode Control**. *Tikrit Journal of Engineering Sciences* 2025; **32**(3): 1548.
http://doi.org/10.25130/tjes.32.3.1

*Corresponding author:

Reyam G. Ghane

Control and Systems Engineering Department, University of Technology, Baghdad, Iraq.

Abstract: The present paper presents the design of a foldable quadrotor that can adapt its morphology in the presence of sudden external disturbances such as wind. It focuses on solving the problem of tracking a specific trajectory of the foldable quadrotor in the presence of external disturbances. Therefore, robust controllers were designed to ensure better tracking under sudden turbulence, such as wind, considering the inertia change due to the rotating arms. An architectural console for foldable quadrotors was introduced under a gust of conservative winds. A dual loop control strategy was used in which the movements in the X and Y axes were managed by a nonlinear PID controller in the outer loop. In addition, a sliding mode controller was added to the inner loop to regulate the attitude and height in the Z direction, where the mechanical model of the aircraft was combined with the conservative wind gust model. When a conservative wind gust hit the foldable quadrotor for a certain period, a slight deviation from the proposed path at the beginning and end of the disturbance existed with an overshoot (7.468×10^{-3}) for the x-axis and (8.069×10^{-2}) for the z-axis at the beginning of the disturbance, while at the end of disturbance on the z-axis appears undershoot in its value (6.725×10^{-2}). Therefore, the quadrotor maintained its stability with an accuracy of 98%.

رفض اضطراب الرياح لمحرك طائرة رباعي قابل للطي باستخدام التحكم في وضع الانزلاق غير الخطي القائم على التناسب-التكامل-التفاضل

ريام غسان غني، محمد يوسف حسن
قسم هندسة السيطرة والنظم / الجامعة التكنولوجية / بغداد - العراق.

الخلاصة

تقدم هذه الورقة تصميمًا رباعيًا قابل للطي يمكنه تكييف شكله في وجود اضطرابات خارجية مفاجئة مثل الرياح. إنه يركز على حل مشكلة تتبع مسار محدد للرباعي القابل للطي في وجود اضطرابات خارجية. لذلك تم تصميم وحدات تحكم قوية لضمان تتبع أفضل في ظل الاضطرابات المفاجئة، مثل الرياح، مع مراعاة تغير القصور الذاتي بسبب دوران الأذرع. تم تقديم وحدة تحكم معمارية للرباعي القابل للطي تحت تأثير هبوب رياح محافظة. يتم استخدام إستراتيجية التحكم في الحلقة المزدوجة حيث تتم إدارة الحركات في المحورين X و Y بواسطة وحدة تحكم PID غير خطية في الحلقة الخارجية. فضلاً عن ذلك تمت إضافة وحدة تحكم في الوضع المنزلق إلى الحلقة الداخلية لتنظيم الموقف والارتفاع في الاتجاه Z، حيث يتم دمج النموذج الميكانيكي للطائرة مع نموذج عاصفة الرياح المحافظة. عندما تضرب عاصفة رياح معتدلة الرباعي القابل للطي لفترة معينة، يوجد انحراف طفيف عن المسار المقترح في بداية ونهاية الاضطراب مع تجاوز (٧.٤٦٨×١٠^{-٣}) للمحور السيني، (٨.٠٦٩×١٠^{-٢}) للمحور z في بداية الاضطراب بينما يظهر في نهاية الاضطراب على المحور z أقل من الهدف في قيمته (٦.٧٢٥×١٠^{-٢}). لذلك، يحافظ المحرك الرباعي على ثباته بدقة تصل إلى ٩٨٪.

الكلمات الدالة: محرك رباعي قابل للطي، التحكم في الوضع الانزلاقي، PID غير الخطي، عاصفة الرياح.

1.INTRODUCTION

The popularity of quadrotors has grown recently. Because of the numerous activities that it conducts difficult for humans to implement. Therefore, it has become an essential platform for scientists and researchers to develop and upgrade. Its tasks range from civilian to military applications, such as research, delivery, and espionage [1]. Much research has been done on this intriguing technology's flight stability [2], [3], in addition to improving the quadrotor used for delivery operations [4, 5]. Due to the stable structure of quadrotors, it will be challenging for them to maneuver through congested and small spaces while conducting tasks. Consequently, many researchers have suggested that a quadrotor that can change its shape in response to obstacles is required, such as using the origami technique or simulating bird flight [6 - 9]. Therefore, controlling the foldable quadrotor became an important challenge to maintaining its stability when changing its morphology during flight, especially under various external disturbances. The control of position and attitude is greatly affected by external disturbances, particularly during wind gusts. Numerous foldable quadrotor control strategies have been researched, such as the Model Reference Adaptive Control model of an X-morphology robot, which effectively adapts to folding maneuvers [10]. Also, a Linear Quadratic Regulator controller was proposed to ensure stable flight [11]. Backstepping was also used as a new control strategy to maintain the stability of a folding quadrotor [12]. However, a few studies have been done on the strong control of the quadrotor, particularly in windy conditions. Alexis et al. [13] proposed a robust predictive control model based on the Piecewise Affine (PWA) and used color noise to generate wind speeds. A mechanical fan was utilized by Cabecinhas et al. [14] to produce turbulence, which they then controlled using a powerful nonlinear adaptive state feedback controller and developed a reliable controller based on a linear active disturbance rejection control to regulate the stability of an aerial robot under windy situations [15]. Also, a controller was designed that combines PID control theory and fuzzy control theory to maintain the position on the desired trajectory in the presence of wind disturbances. This controller aims to create a continuously variable function between the PID parameters, the absolute error value, and the absolute error value changes [16]. A simple control unit consisting of a PD for the attitude and a PID for the position is designed, which is done to keep the quadrotor stable in the presence of persistent and variable wind disturbances [17]. To deal with some external disturbances that affect quadrotor dynamics, such as the effect of wind, several researchers developed an intelligent control method based on neural networks. A set of PID controllers works with an adaptive neuromas estimator and an adaptive neural disturbance estimator to stabilize the quadrotor and enhance system performance [18]. A robust nonlinear control strategy was proposed based on the double loop system that combines integral sliding mode and backstepping sliding mode controllers to adapt the tracking to the required position under uncertain situations and when there are disturbances like wind disturbances [19]. For a quadrotor model subject to wind turbulence, load change, or rotor efficiency loss, several researchers proposed a predictive algorithm-based observer method combined with robust control designs to compensate for intermediate responses, such as delays in the velocities change rate and settling time [20]. To improve the performance of trajectory tracking and problem-solving, the researchers suggested a dual loop single-dimension fuzzy sliding mode control technique, with the design of a disturbance observer in feedback. The simulation results showed the robustness of the proposed algorithm against disturbances [21]. The predictive sliding mode control technique was

designed to concurrently reject sudden stochastic disturbances (wind turbulence) and time-variant parametric uncertainty. To represent wind turbulence, the Dryden discrete turbulence model was used as a baseline [22]. A fault tolerance control system is also employed to preserve stability, lessen performance degradation, and compensate for system component failures [23]. Additionally, it was suggested to use Embedded Design Techniques (EDTs) in designing a PID controller to achieve stability and lower hardware and cost [24]. In the present research, the focus is on tracking the trajectory of the foldable quadrotor in the presence of external disturbances problem. To ensure good tracking for the foldable quadrotor under the effect of turbulence, such as wind, inner and outer loop controllers are proposed. A nonlinear PID controller is designed in the outer loop, and a sliding mode controller is added to the inner loop. The design considers the variation of inertia due to the rotating arms. It is noted that although the foldable quadrotor was a highly coupling model, the proposed control units succeeded in keeping the foldable quadrotor to follow the proposed path under the influence. This paper is structured as follows: Section 2 explains the quadrotor's mechanical architecture and considers its center of gravity. Section 3 presents the proposed control unit plan. Section 4 demonstrates the effect of wind on the quadrotor and the effectiveness of the proposed controller. Section 5 fully describes the simulation findings. Section 6 summarizes the conclusions.

2.MODELING OF A FOLDABLE QUADROTOR

Figure 1 shows the foldable quadrotor consisting of a fixed central body of mass m_o and four arms of a masses $m_{2,i}$ foldable around the central body at different angles (see Table 1) [25]. The folding arms were connected to these servo motors of masses $m_{1,i}$, while these motors were directly connected to the central body. The possible shapes for this foldable quadrotor are (X, H, O, Y, YI, and T). By calculating the control matrix for each shape, the various angles represent the extent of the folded arms [26]. There were also four rotors of masses $m_{3,i}$ on the arms. Rotors 2 and 4 rotated clockwise, while rotors 1 and 3 rotated counterclockwise. The servo motors changed the quadrotor's shape, resulting in a strongly coupled system. The arms and rotors revolved on the same axis as the main body, fixed around the Z-axis. Therefore, adjusting the position of the arms, the most (traditional) setup, led to a wide range of possible shapes [25]. To make a suitable model for the foldable quadrotor, the following assumptions are stated [27]:

1- The rotation arms, servo motors, and central body are rigid.
2- Assuming that the propeller is stiff, the impact of its changing morphology during flight is disregarded.

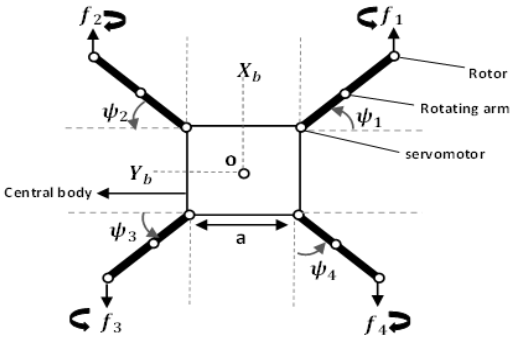

Fig. 1 Schematic of the Foldable Quadrotor [25].

Table 1 Characteristics of the Foldable Quadrotor Configuration [26].

Configuration	Arm angles			
	$\psi_1(t)$	$\psi_2(t)$	$\psi_3(t)$	$\psi_4(t)$
X	$\pi/4$	$\pi/4$	$\pi/4$	$\pi/4$
H	$\pi/2$	0	$\pi/2$	0
O	π	π	π	π
Y	$\pi/4$	$\pi/4$	$\pi/2$	0
YI	$\pi/2$	0	$\pi/4$	$\pi/4$
T	0	$\pi/2$	$\pi/2$	0

The Newton-Euler approach was used to derive the dynamic of the quadrotor, which depends on the fixed body frame and the mobile frame, to derive the translational dynamic and the rotational equations. From Fig. 1, the four rotors represent four input forces, essentially representing the thrust produced by each propeller. The sum of each motor's thrusts is the collective input (U_1). Pitch moment is obtained by raising (or decreasing) the rear motor's speed while decreasing (or increasing) the front motor's speed. By increasing (or decreasing) the speed of the right motor while decreasing (or raising) the speed of the left motor, the roll movement is produced. By jointly increasing (or decreasing) the speed of the front and rear motors while lowering (or raising) the speed of the lateral motors collectively, the yaw movement is produced [28]. The dynamic of a foldable quadrotor is derived using Newton-Euler formalism. The equations that describe those dynamics are [26]:

$$\ddot{x} = \frac{\sin\psi\sin\varphi + \cos\psi\sin\theta\cos\varphi}{m}U_1 + \frac{-k_{Dx}}{m}\dot{x} \quad (1)$$

$$\ddot{y} = \frac{\sin\psi\sin\theta\cos\varphi - \cos\psi\sin\varphi}{m}U_1 + \frac{-k_{Dy}}{m}\dot{y} \quad (2)$$

$$\ddot{z} = \frac{\cos\varphi\cos\theta}{m}U_1 - g + \frac{-k_{Dz}}{m}\dot{z} \quad (3)$$

$$\ddot{\varphi} = \frac{J_{yy} - J_{zz}}{J_{xx}}\dot{\theta}\dot{\psi} + \frac{-J_r}{J_{xx}}\dot{\theta}\Omega_r + \frac{1}{J_{xx}}U_2 + \frac{-k_{Ax}}{J_{xx}}\dot{\varphi}^2 \quad (4)$$

$$\ddot{\theta} = \frac{J_{zz} - J_{xx}}{J_{yy}}\dot{\varphi}\dot{\psi} + \frac{J_r}{J_{yy}}\dot{\varphi}\Omega_r + \frac{1}{J_{yy}}U_3 + \frac{-k_{Ay}}{J_{yy}}\dot{\theta}^2 \quad (5)$$

$$\ddot{\psi} = \frac{J_{xx} - J_{yy}}{J_{zz}}\dot{\varphi}\dot{\theta} + \frac{1}{J_{zz}}U_4 + \frac{-k_{Az}}{J_{zz}}\dot{\psi}^2 \quad (6)$$

where (x, y, z) represents the quadrotor's position in the mobile frame, and (φ, θ, ψ) represents the roll, pitch, and yaw caused by the fixed body frame, i.e., the gyroscopic effect. The state space vector for the nonlinear dynamic model based on the basic equations is given by [26]:

$$\mathbf{an\ X} = [\mathrm{x}\ \dot{\mathrm{x}}\ \mathrm{y}\ \dot{\mathrm{y}}\ \mathrm{z}\ \dot{\mathrm{z}}\ \varphi\ \dot{\varphi}\ \theta\ \dot{\theta}\ \psi\ \dot{\psi}]^T \quad (7)$$

Also, the state space vector is written as [26]:

$$\mathbf{X} = [x_1\ x_2\ x_3\ x_4\ x_5\ x_6\ x_7\ x_8\ x_9\ x_{10}\ x_{11}\ x_{12}]^T \quad (8)$$

$$\begin{cases} \dot{x}_1 = x_2 \\ \dot{x}_2 = U_1\dfrac{u_x}{m} + b_1 x_2 \\ \dot{x}_3 = x_4 \\ \dot{x}_4 = U_1\dfrac{u_y}{m} + b_2 x_4 \\ \dot{x}_5 = x_6 \\ \dot{x}_6 = -g + U_1\dfrac{\cos\varphi\cos\theta}{m} + b_3 x_6 \\ \dot{x}_7 = x_8 \\ \dot{x}_8 = a_1\dot{\theta}\dot{\psi} + a_4\dot{\theta}\Omega_r + \dfrac{1}{J_{xx}}U_2 + b_4\dot{\varphi}^2 \\ \dot{x}_9 = x_{10} \\ \dot{x}_{10} = a_2\dot{\varphi}\dot{\psi} + a_5\dot{\varphi}\Omega_r + \dfrac{1}{J_{yy}}U_3 + b_5\dot{\theta}^2 \\ \dot{x}_{11} = x_{12} \\ \dot{x}_{12} = a_3\dot{\varphi}\dot{\theta} + \dfrac{1}{J_{zz}}U_4 + b_6\dot{\psi}^2 \end{cases} \quad (9)$$

where

$a_1 = \frac{J_{yy}-J_{zz}}{J_{xx}}$, $a_2 = \frac{J_{zz}-J_{xx}}{J_{yy}}$, $a_3 = \frac{J_{xx}-J_{yy}}{J_{zz}}$, $a_4 = \frac{-J_r}{J_{xx}}$, $a_5 = \frac{J_r}{J_{yy}}$

$b_1 = \frac{-k_{Dx}}{m}$, $b_2 = \frac{-k_{Dy}}{m}$, $b_3 = \frac{-k_{Dz}}{m}$, $b_4 = \frac{-k_{Ax}}{J_{xx}}$, $b_5 = \frac{-k_{Ay}}{J_{yy}}$, $b_6 = \frac{-k_{Az}}{J_{zz}}$

$$u_x = \sin\Psi\sin\varphi + \cos\Psi\sin\theta\cos\varphi \quad (10)$$

$$u_y = \sin\Psi\sin\theta\cos\varphi + \cos\Psi\sin\varphi \quad (11)$$

$$\Omega_r = \Omega_1^2 - \Omega_2^2 + \Omega_3^2 - \Omega_4^2 \quad (12)$$

where $J_{(xx,yy,zz)}$ is the moment of inertia, J_r is the rotor inertia, $k_{D(x,y,z)}$ are the translation drag coefficients, $k_{A(x,y,z)}$ are the aerodynamic friction coefficients, Ω_i is the rotor speed for every arm, g is the gravity, m is the mass of the foldable quadrotor, and $\psi_i(t)$ is the angle for every arm of the foldable quadrotor where $i = 1, 2, 3, 4$.

3.CONTROL DESIGN FOR THE FOLDABLE QUADROTOR

Due to the foldable quadrotor's nonlinear, underactuated, and strongly coupled, a double-loop design approach was used to construct the controller (see Fig. 2). Use the controller in sliding mode in the inner loop because it provides a reliable layout to ensure the stability of the controller and follow the suggested path [29]. Since there are no real (XY) motion control inputs in the quadrotor system, the nonlinear PID generates the appropriate control signals in the (XY) plane, as it is more flexible in dealing with nonlinear systems [30].

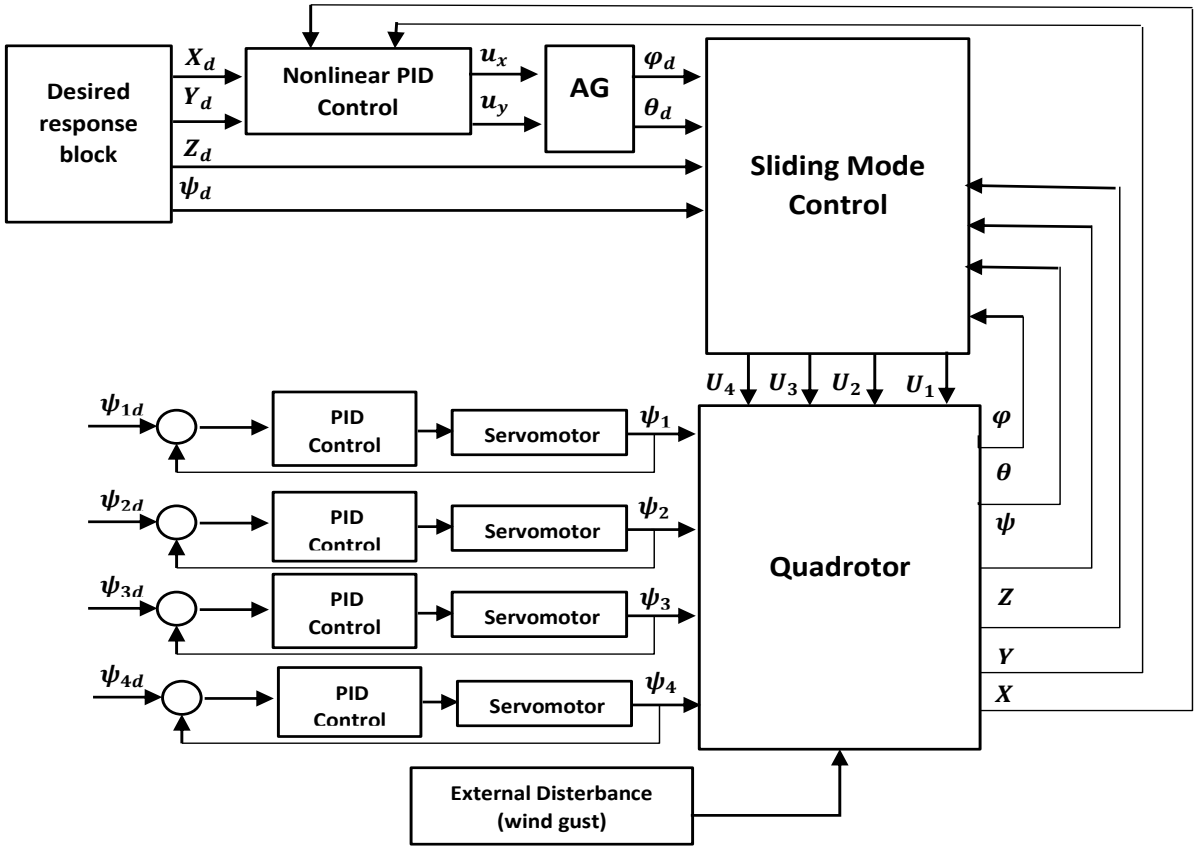

Fig. 2 Proposed Foldable Quadrotor Control Design under Wind Gusts.

where AG means Angle Generation (to generate the desired angle).

3.1.Design of Inner Loop Sliding Mode Control

For the altitude (Z) [26]:

$$\begin{cases} \dot{x}_5 = x_6 \\ \dot{x}_6 = -g + U_1 \dfrac{\cos\varphi \cos\theta}{m} + b_3 x_6 \end{cases} \quad (13)$$

The tracking error of the altitude e_5 is expressed as:

$$e_5 = x_5 - x_{5d} \quad (14)$$

where x_5 is the actual altitude, and x_{5d} is the desired altitude. The sliding surface for the altitude is:

$$s_5 = \dot{e}_5 + c_5 e_5 \quad (15)$$

Taking the derivative of the sliding surface:

$$\dot{s}_5 = \ddot{e}_5 + c_5 \dot{e}_5 \quad (16)$$

To guarantee $\dot{s}_5 = 0$, the U_1 must be:

$$U_1 = \frac{m}{cosx_7 cosx_9}[\ddot{x}_{5d} + g - b_3 x_6 - c_5(x_6 - \dot{x}_{5d}) - k_5 sgn(s_5) - k_6 s_5] \quad (17)$$

Repeat the same above steps to find the control signal for the attitude ($\varphi, \theta, and\ \psi$), so:

$$an\ U_2 = J_{xx}[\ddot{x}_{7d} - a_1 x_{10} x_{12} - a_4 x_{10}\Omega_r - b_4 x_8^2 - c_7(x_8 - \dot{x}_{7d}) - k_7 sgn(s_7) - k_8 s_7] \quad (18)$$

$$U_3 = J_{yy}[\ddot{x}_{9d} - a_2 x_8 x_{12} - a_4 x_8 \Omega_r - b_5 x_9^2 - c_9(x_{10} - \dot{x}_{9d}) - k_9 sgn(s_9) - k_{10} s_9] \quad (19)$$

$$U_4 = J_{zz}[\ddot{x}_{11d} - a_3 x_8 x_{10} - b_6 x_{12}^2 - c_{11}(x_{12} - \dot{x}_{11d}) - k_{11} sgn(s_{11}) - k_{12} s_{11}] \quad (20)$$

Figure 3 shows the MATLAB/Simulink model for designing a sliding mode control. Equations (17) – (20) describe the four input signals for control. The signal U_1 is used to ensure that the height follows the reference value, while signals U_2, U_3, and U_4 are used to regulate the pitch, yaw, and roll of the system.

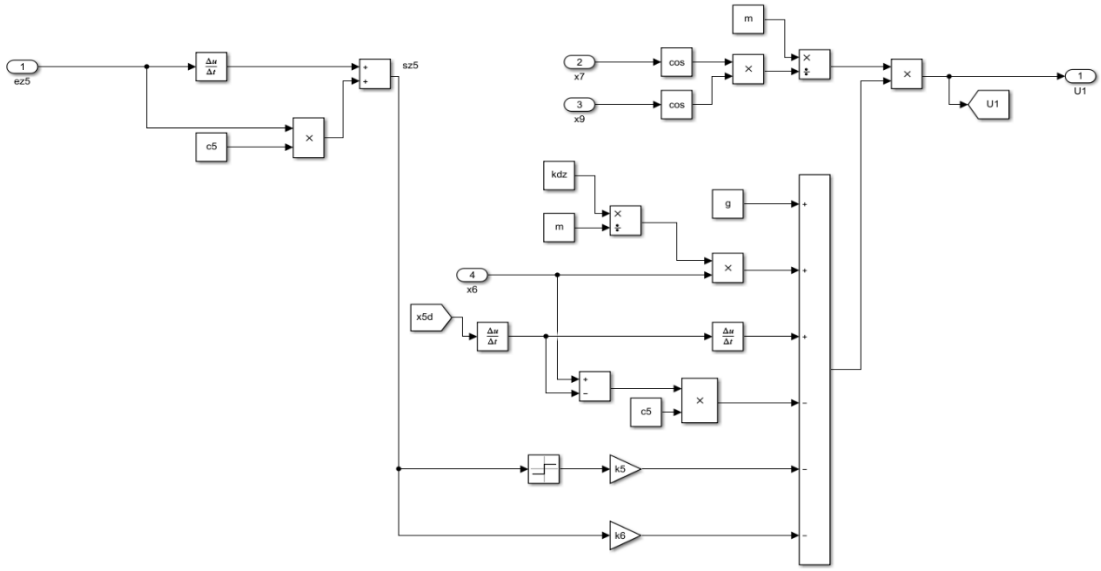
1
ez5
c5
sz5
2
x7
3
x9
cos
cos
m
U1
1
U1
kdz
m
g
4
x6
x5d
c5
k5
k6

(a)

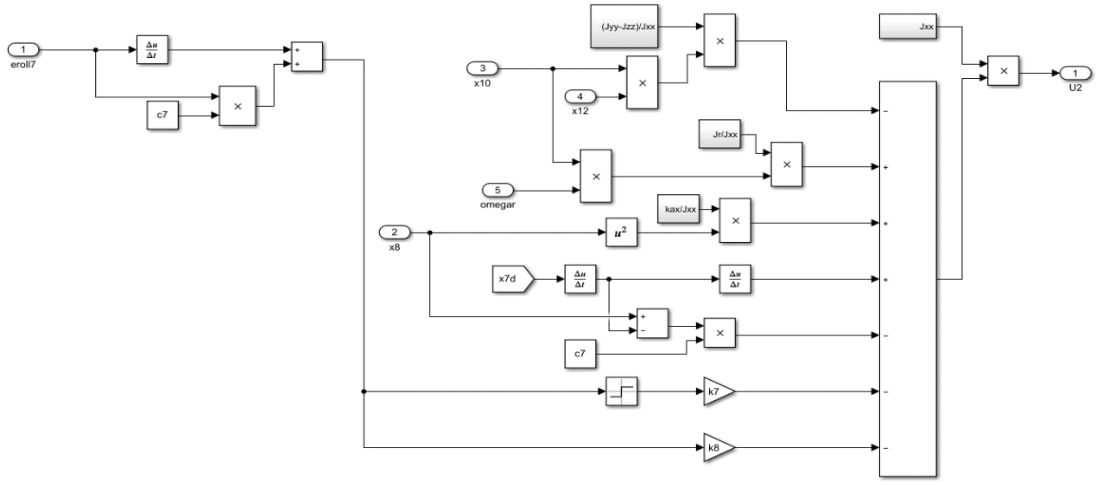
1
eroll7
c7
(Jyy-Jzz)/Jxx
3
x10
4
x12
Jxx
1
U2
Jr/Jxx
5
omegar
kax/Jxx
2
x8
x7d
c7
k7
k8

(b)

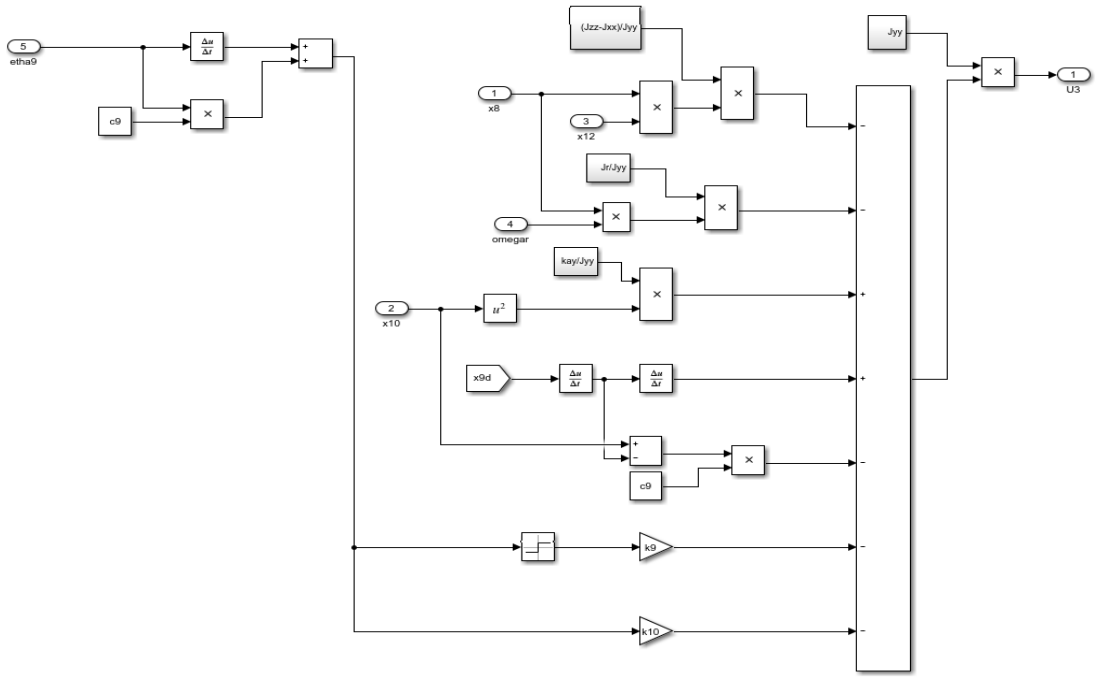
5
etha9
c9
(Jzz-Jxx)/Jyy
Jyy
1
U3
1
x8
3
x12
Jr/Jyy
4
omegar
kay/Jyy
2
x10
x9d
c9
k9
k10

(c)

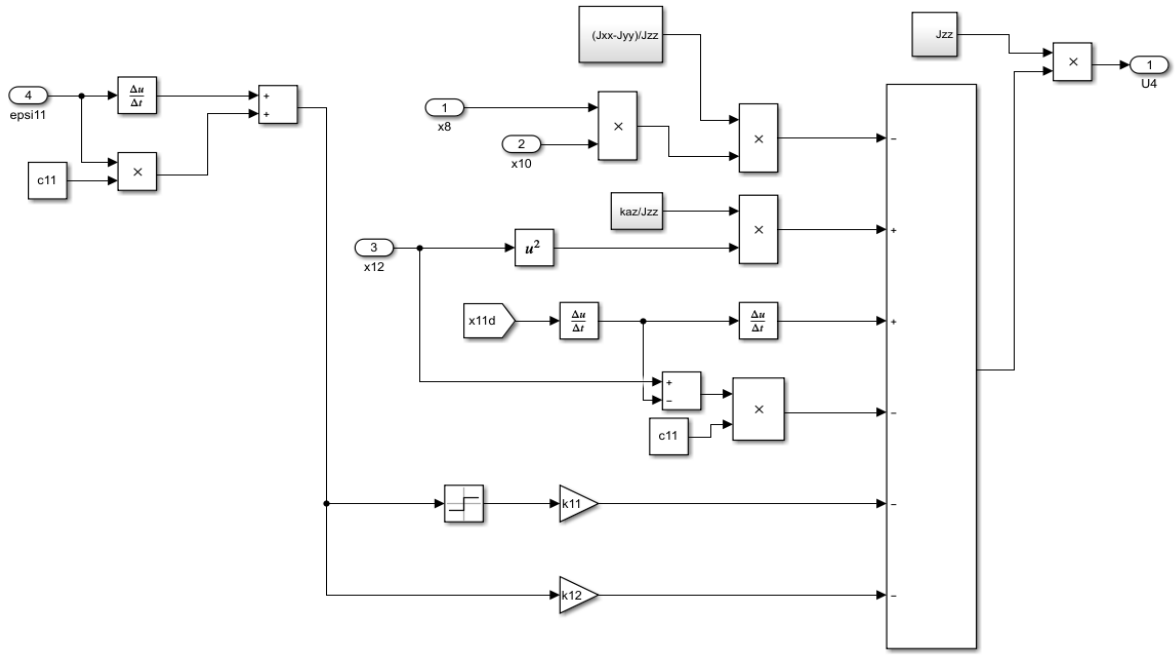

(d)

Fig. 3 Simulink Model of the Sliding Mode Control: (a) Simulink Model for U_1, (b) Simulink Model for U_2, (c) Simulink Model for U_3, and (d) Simulink Model for U_4.

3.2.Design of Outer Loop Nonlinear PID Control

A quadrotor system has no real control inputs for movement in the (X, Y) plane. To generate a control signal (u_x u_y) suitable for movement in the (X, Y) plane, the following analysis is recommended [26]. By solving Eqs. (10) and (11), compute the desired roll and desired pitch:

$$\varphi_d = \text{asin}(u_x sin\psi_d - u_y cos\psi_d) \quad (21)$$

$$\theta_d = \text{asin}\left(\frac{u_x cos\psi_d + u_y sin\psi_d}{cos\varphi_d}\right) \quad (22)$$

The two equations above represent the desired values for roll and pitch angles. The conventional PID has been improved to offer more freedom. As demonstrated in the equations below, it was rebuilt by substituting the linear PID parts with nonlinear functions:

$$\begin{cases} U_{NLPID} = f_p(e) + f_d(\dot{e}) + f_i(\int e dt) \\ f_i = k_i(\varepsilon)|\varepsilon|^{\alpha_i} sign(\varepsilon), \quad \varepsilon = e, \dot{e}, \int e \\ k_i(\varepsilon) = k_{i1} + \frac{k_{i2}}{1+\exp(\mu_i \beta^2)}, i = p, d, i \end{cases} \quad (23)$$

The NLPID controller's main goal is to make the (X and Y) position error approaches zero, so the appropriate control signals in the (X, Y) plane are:

$$u_x = \frac{m}{U_1}[\frac{k_{dx}}{m} x_2 + \ddot{x}_{1d} - f_{x1}(e_x) - f_{x2}(\dot{e}_x) + f_{x3}(\int e_x dt)] \quad (24)$$

$$u_y = \frac{m}{U_1}[\frac{k_{dy}}{m} x_4 + \ddot{x}_{3d} - f_{y1}(e_y) - f_{y2}(\dot{e}_y) + f_{y3}(\int e_y dt)] \quad (25)$$

4.DISTURBANCE REJECTION SCHEME FOR PROPOSED CONTROLLER DESIGN

In the nonlinear controller's design, the impact of interactions between several axes must be considered. The quadrotor model is combined with the wind turbulence model. The basic idea is to build a sliding surface and ensure that it reaches the origin point (s=0), achieved by ensuring ($s\dot{s} < 0$), to achieve strong stability, reject external disturbances, and make the response of the quadrotor close to the target desired. The model used to simulate wind turbulence is a conservative wind gust model, represented by the speed equations below [31]:

$$v_x = t - a * cos(t) \quad (26)$$

$$v_y = b * t \quad (27)$$

$$v_z = t - a * cos(t) * \text{sin}(t) \quad (28)$$

where a and b represent the input amplitude coefficients, which have a role in enlarging the sinusoids for the x and z axes and increasing the speed for the time for the y-axis, meaning that the proposed wind speed is integrated with the speed of the quadrotor.

5.STABILITY ANALYSIS

In this section, the stability of the inner and outer rings will be analyzed. Lyapunov theory will be used to analyze the stability of the inner loop, while the Ruth Horowitz stability criterion will be used on the linear model with virtual controllers for both X and Y motion.

5.1.Lyapunov Stability Analysis

Let $\dot{x} = f(x), x = 0$, and $D \in R^n$ be a domain that contains $x = 0$, whereas $v: D \to R$. Let v be a Lyapunov function, which is stickily positive definite and chosen as follows:

$$v(s_i) = \frac{1}{2}s_i^2, for\ i = 5,7,9,11 \quad (29)$$

A sufficient condition for stability is guaranteed if the derivative of the Lyapunov function is negative definite ($\dot{v}(s_i) < 0$). So, take the time derivative for Eq. (29):

$$\dot{v}(s_i) = s_i\dot{s}_i < 0 \quad (30)$$

Since the constant reaching law is given as follows:

$$\dot{s}_i = -k_1 sgn(s_i) - k_2 s_i \quad (31)$$

By substituting Eq. (31) in Eq. (30).

$$\dot{s}_i = -k_1 sgn(s_i) - k_2 s_i \quad (32)$$

The Lyapunov theorem is satisfied with the domain term if ($k_2 s_i^2 > 0$, $k_1 > 0$, and $\forall s_i \neq 0$) to ensure that the trajectories are globally asymptotically tracked in their desired positions.

5.2.Routh Hurwitz Stability Analysis

The linear system of motion in the (X, Y) plane of the quadrotor is represented as follows:

$$\begin{cases} \dot{x}_1 = x_2 \\ \dot{x}_2 = u_x \\ \dot{x}_3 = x_4 \\ \dot{x}_4 = u_y \end{cases} \quad (33)$$

where $x = \{x, \dot{x}, y, \dot{y}\}$. So, the subsystem shown in Eq. (33) can be represented in the following general terms:

$$\begin{cases} \dot{\beta}_1 = \beta_2 \\ \dot{\beta}_2 = u_\beta \end{cases} \quad (34)$$

Be representing subs $\beta_1 = x_i$, $\beta_2 = x_{i+1}$ for $i = [1,3]$, $u_\beta = [u_x, u_y]$. So, to prove the stability of the x and y motion of the quadrotor, all α in Eq. (23) approximate 1, leading to ($|\varepsilon|sign(\varepsilon) = \varepsilon$). Let the errors of the closed-loop system for X and Y motion can be represented by:

$$\begin{cases} e_o = \int e_1 dt \\ e_1 = \beta_{1d} - \beta_1 \\ e_2 = \dot{\beta}_{1d} - \beta_2 = \beta_{2d} - \beta_2 \end{cases} \quad (35)$$

Taking derivative:

$$\begin{cases} \dot{e}_o = e_1 \\ \dot{e}_1 = e_2 \\ \dot{e}_2 = -u_\beta \end{cases} \quad (36)$$

By substituting Eq. (23) in Eq. (36), yield:

$$\begin{bmatrix} \dot{e}_o \\ \dot{e}_1 \\ \dot{e}_2 \end{bmatrix} = \begin{bmatrix} 0 & 1 & 0 \\ 0 & 0 & 1 \\ -k_i(e_o) & -k_p(e_1) & -k_d(e_2) \end{bmatrix} \begin{bmatrix} e_o \\ e_1 \\ e_2 \end{bmatrix} =$$

$$\begin{bmatrix} \dot{e}_o \\ \dot{e}_1 \\ \dot{e}_2 \end{bmatrix} = A \begin{bmatrix} e_o \\ e_1 \\ e_2 \end{bmatrix} \quad (37)$$

Taking $|\lambda I - A| = 0$, to find the characteristics equation:

$$\lambda^3 + \lambda^2 k_d(e_2) + \lambda k_p(e_1) + k_i(e_o) = 0 \quad (38)$$

from Eq. (38), find the Hurwitz Matrix:

$$H = \begin{bmatrix} k_d(e_2) & k_i(e_o) & 0 \\ 1 & k_p(e_1) & 0 \\ 0 & k_d(e_2) & k_i(e_o) \end{bmatrix} \quad (39)$$

For the Hurwitz matrix to be stable, it must be $k_d(e_2) > 0$, $k_d(e_2)k_p(e_1) - k_i(e_o) > 0$, $k_p(e_1)k_d(e_2)k_i(e_o) - k_i^2(e_o) > 0$

Since $k_i(\varepsilon) \in \left\{k_{i1}, k_{i1} + \frac{k_{i2}}{2}\right\}$ and always be positive. Let $k_p(e_1) \in \left\{k_{p1}, k_{p1} + \frac{k_{p2}}{2}\right\}$ and $k_i(e_o) \in \left\{k_{i1}, k_{i1} + \frac{k_{i2}}{2}\right\}$ resulting in $k_d(e_2) > \frac{k_i(e_o)}{k_p(e_1)}$ giving $k_{d1} > \frac{k_{i1}}{k_{p1} + \frac{k_{p2}}{2}}$ and $k_{d1} + \frac{k_{d2}}{2} > \frac{k_{i1} + \frac{k_{i2}}{2}}{k_{p1}}$

As a result, the closed-loop system stability by Hurwitz's stability theory will be ensured.

6.SIMULATION RESULTS

The six degrees of freedom nonlinear system model and the proposed controllers for this quadrotor are simulated using MATLAB/Simulink. This folding quadrotor is simulated under external turbulence (a conservative model of a simulated wind) effects. The values of the parameters used in the simulation are listed in Table 2 [25] and Table 3 [31]. Since this type of quadrotor significantly influences the inertia matrix, each case has a certain inertia value, as shown in Table 4 [25].

Table 2 Foldable Quadrotor Parameters [25].

Parameters	Description	Value
m	Mass platform	1133g
g	Gravity	9.81
l	Length of arm	21cm
d	Drag coefficient	1.61×10^{-4}
b	Thrust coefficient	6.317×10^{-4}

Table 3 The Parameters of the Wind Gust Model [31].

Parameters	Value
a	15
b	1

Table 4 The Possible Inertia Values for Each Shape [25].

Configuration	$J_{xx}(kg.m^2)$	$J_{yy}(kg.m^2)$	$J_{zz}(kg.m^2)$
X	1.211×10^{-2}	1.213×10^{-2}	2.370×10^{-2}
H	2.888×10^{-3}	1.978×10^{-2}	2.112×10^{-2}
O	4.719×10^{-3}	7.743×10^{-3}	7.491×10^{-3}
Y	7×10^{-3}	1.597×10^{-2}	2.241×10^{-2}
YI	7×10^{-2}	1.597×10^{-2}	2.241×10^{-2}
T	1.082×10^{-2}	1.084×10^{-2}	2.112×10^{-2}

The parameters of the nonlinear PID and Sliding Mode controllers for the foldable quadrotor are listed in Tables 5 and 6, respectively. These values were obtained using the Firefly evolution algorithm.

Table 5 Parameters for Nonlinear PID Controller.

parameter	value	parameter	value	parameter	value
k_{11x}	3.0151	y_{3x}	0.01	k_{31y}	1.0242
k_{12x}	1.2504	a_{1x}	0.01	k_{32y}	2.5960
k_{21x}	4	a_{2x}	0.3450	y_{1y}	1.9688
k_{22x}	2.0480	a_{3x}	1.3632	y_{2y}	0.01
k_{31x}	0.1105	k_{11y}	4	y_{3y}	3.7522
k_{32x}	1.9498	k_{12y}	2.8314	a_{1y}	0.01
y_{1x}	2.5793	k_{21y}	3.1710	a_{2y}	1.9894
y_{2x}	0.01	k_{22y}	0.01	a_{3y}	0.8624

Table 6 Parameters for Sliding Mode Controller.

Parameters	Value
k_5	4
k_6	4
k_7	3.5165
k_8	0.01
k_9	0.01
k_{10}	0.01
k_{11}	0.01
k_{12}	0.3410

A circular trajectory was used to study the control unit designed for a foldable quadrotor to achieve the required trajectory. The quadrotor flights forward at the height of 6m from the initial position (X, Y, Z) = (0,0,0) and then moves in a closed circular path with a diameter of 3m. The details of the trajectory are shown in Table 7.

Table 7 Circular Trajectory Parameters.

State	Reference Trajectory
X	$\cos(1.5\pi t)$
Y	$sin(1.5\pi t)$
Z	$5u(t)$

The following figures illustrate the simulation results, performed using MATLAB/Simulink with a time setting of 70 seconds. Figure 4 represents the response trajectory for the X, Y, and Z axes under the wind effect and the response for the yaw angle. The windows in Fig. 4 explained the wind effects applied on the quadrotor while tracing the trajectory. Figures 4 (a, b, c) represent the reference and actual trajectories in the X, Y, and Z axes. Figure (4.d) represents the reference and actual trajectory for the yaw angle. Moreover, Fig. 5 illustrates the 3D trajectory for X, Y, and Z tracked by the foldable quadrotor. Figures 6 (a) and (d) show the error between the desired and actual paths of the foldable quadrotor for the X, Y, and Z axes and Yaw angle, respectively. Also, Figs. 7 (a) and (d) represent the four controller signals that control the foldable quadrotor motors. Figures 8 (a) and (d) show the change in the angle values of the four arms by the servomotors.

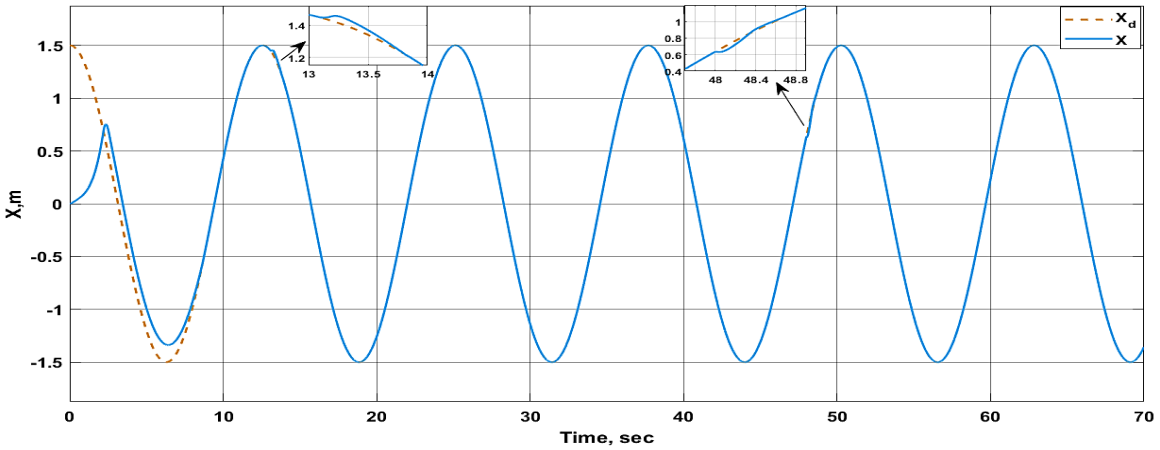

(a)

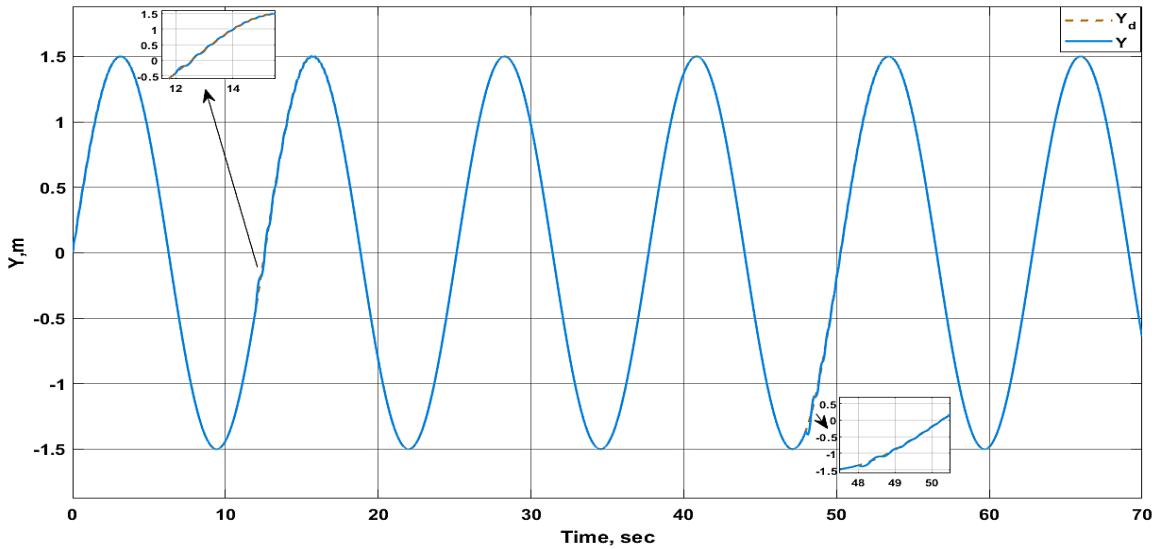

(b)

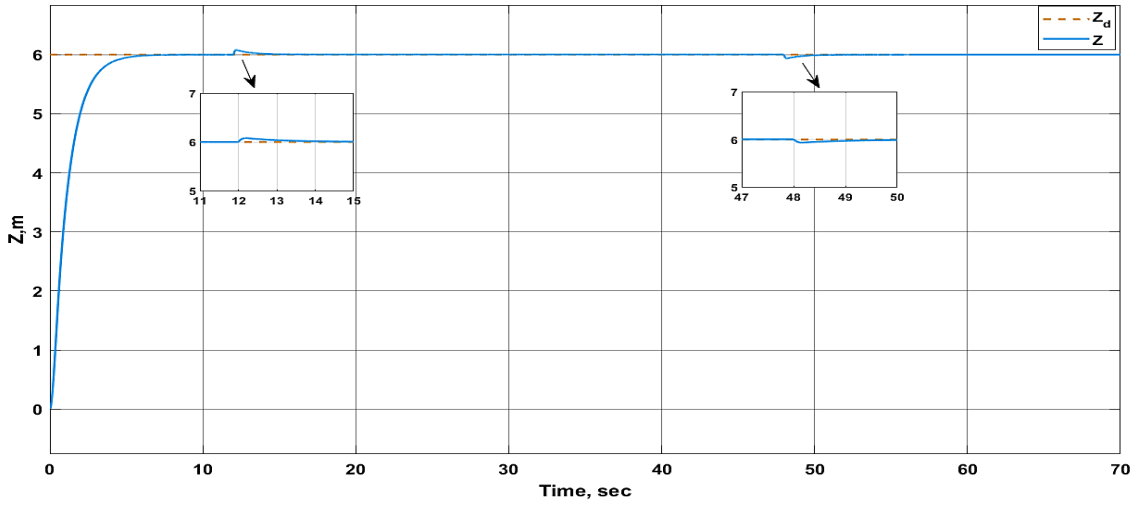

(c)

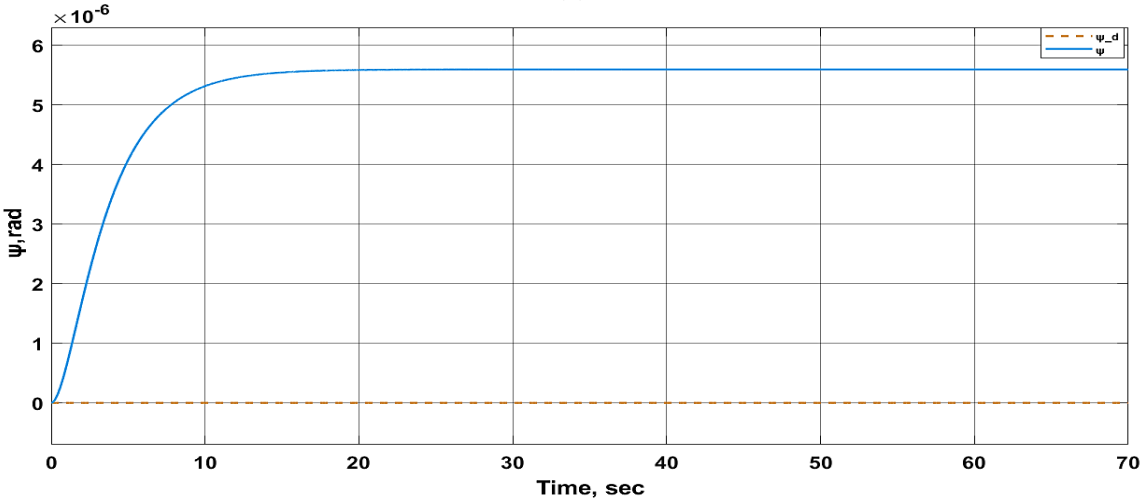

(d)

Fig. 4 The Response of the Position and Yaw Angle Under External Disturbance: (a) X Trajectory, (b) Y Trajectory. (c) Z Trajectory. (d) Yaw Angle.

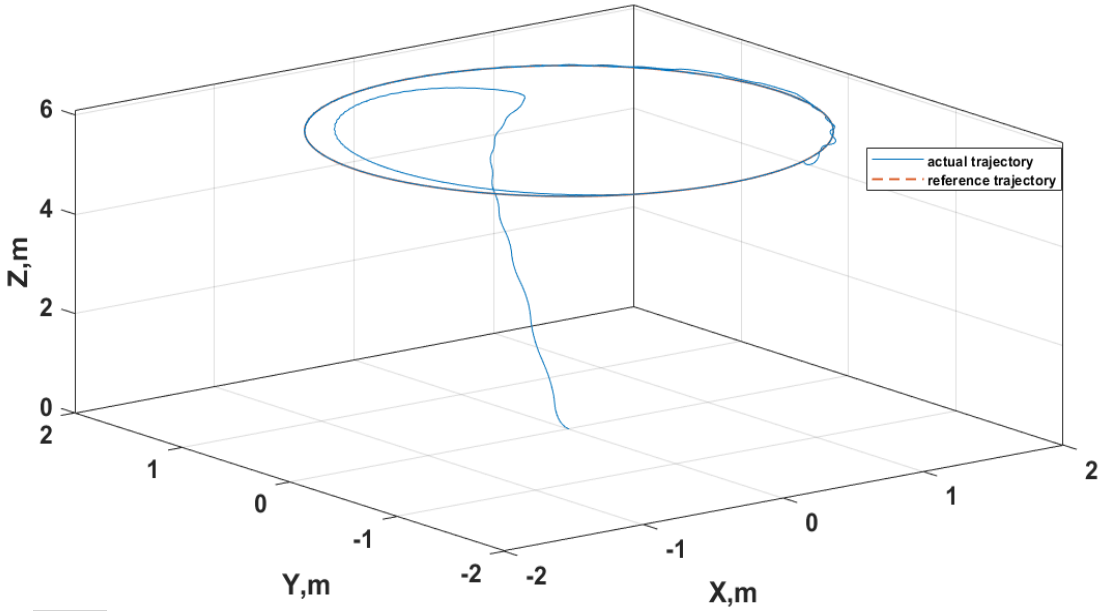

Fig. 5 A Circular Trajectory Control of a Foldable Quadrotor under external disturbance.

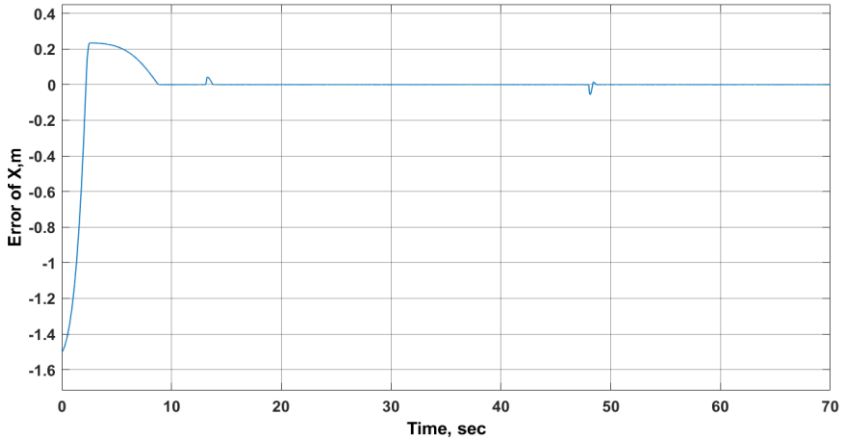

(a)

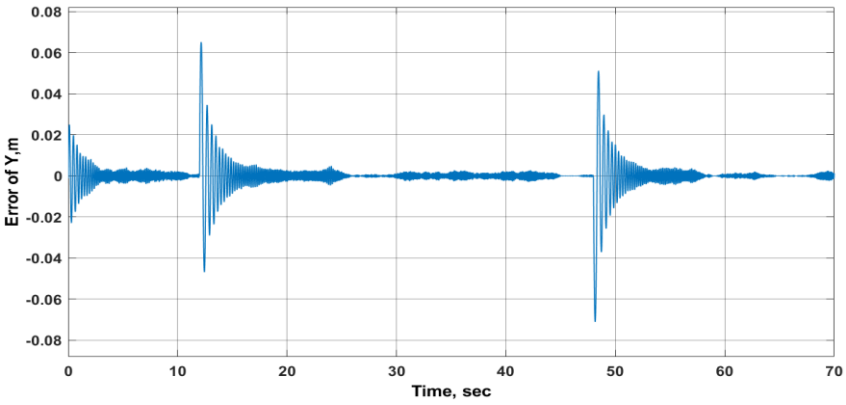

(b)

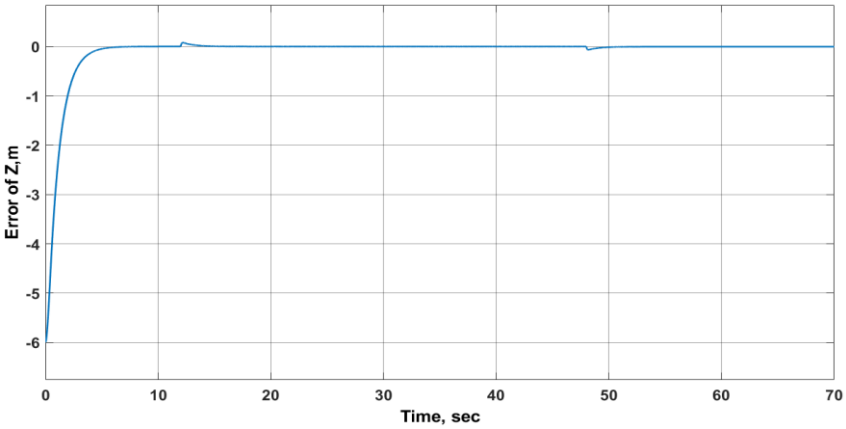

(c)

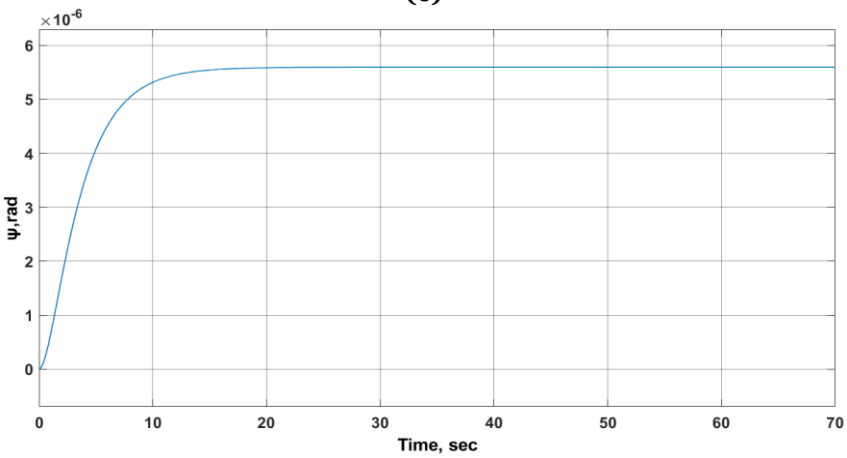

(d)

Fig. 6 Tracking Error in Position and Yaw Angle: (a) Tracking Error in X Position, (b) Tracking Error in Y Position, (c) Tracking Error in Z Position, and (d) Tracking Error in Yaw Angle.

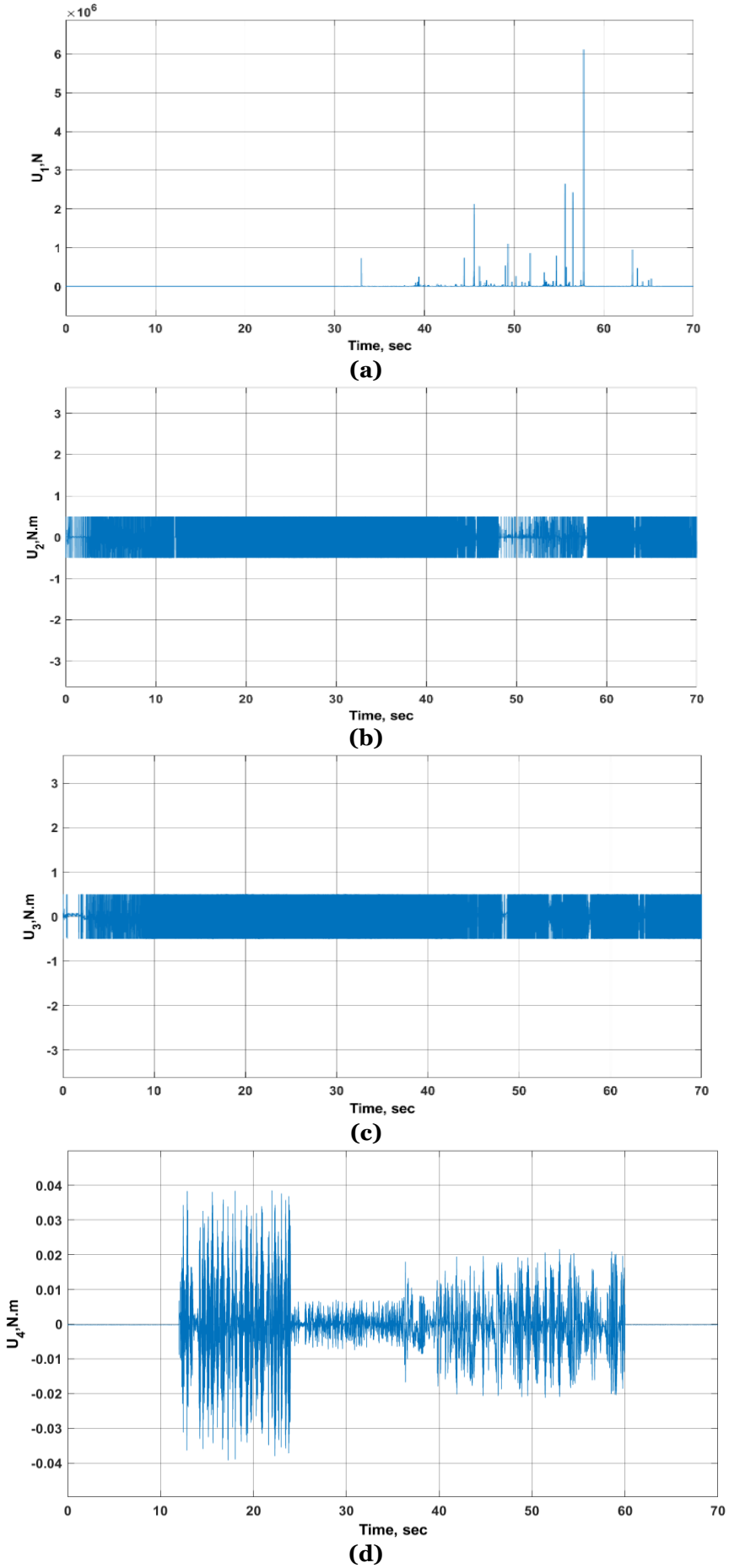

Fig. 7 Control Signals. (a) Evolution of the Command U_1, (b) Evolution of the Command U_2, (c) Evolution of the Command U_3, and (d) Evolution of the Command U_4.

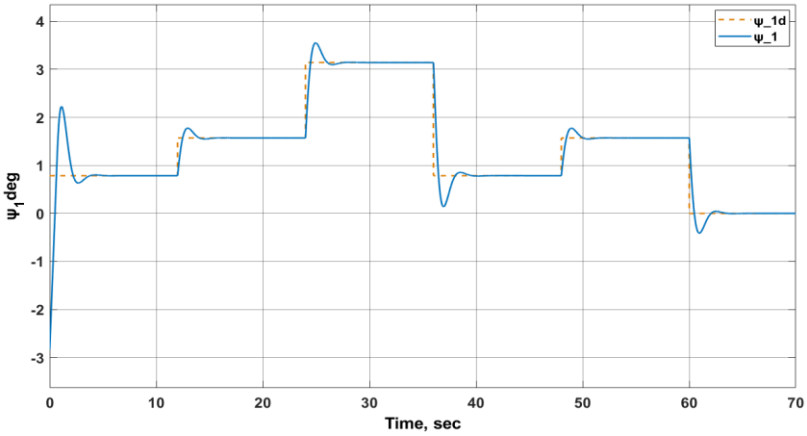

(a)

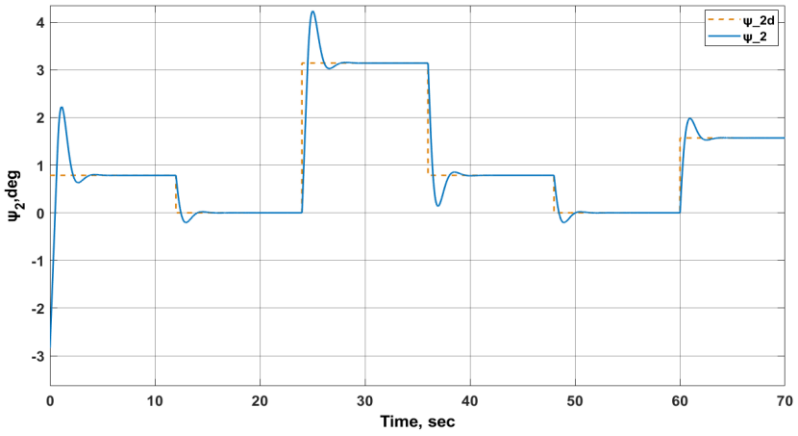

(b)

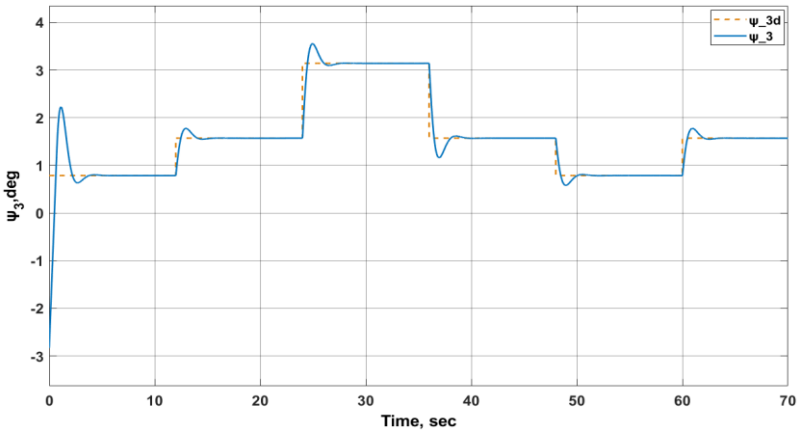

(c)

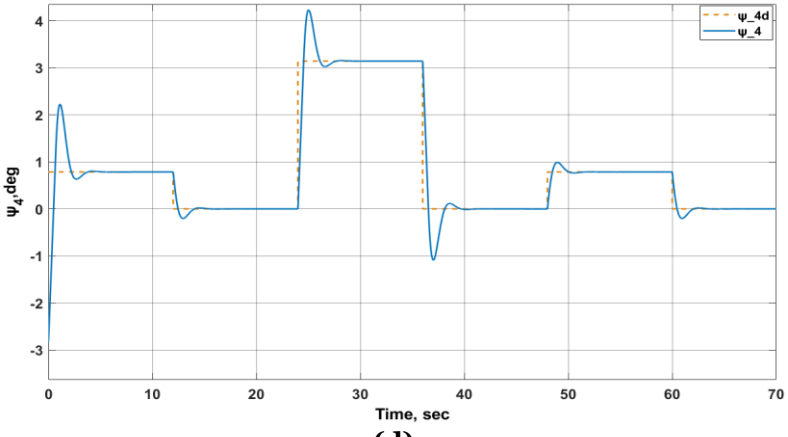

(d)

Fig. 8 Servomotor's Angle Variations: (a) First Arm Angle ψ_1, (b) Second Arm Angle ψ_2, (c) Third Arm Angle ψ_3, and (d) Fourth Arm Angle ψ_4.

A closed circular path was used to study the effect of external winds on the foldable quadrotor. A conservative-type wind model was simulated and added to the velocity after 12 seconds from the start of the flight. The plane's maximum value of the projected wind gust was (1 m/ s). The results are shown in Figs. 4 to 8. It is noticed from Figs. 4 and 5 that the quadrotor showed good tracking of the specified path with few overshoots at the beginning and end of the wind shedding. It maintained stability even during the change of morphology under the influence of wind, as this quadrotor changed its configuration to six configurations, as shown in Table 1 [24, 6], indicating its suitability for working in real different environments. Figure 6 proves that the errors were close to zero with a few excesses at the beginning and the end of the wind blowing, which is evidence of the efficiency of the proposed controller in maintaining the stability of the quadrotor and tracking the path while changing shapes under the influence of sudden winds. Figure 7 presents the control signals. It is noted that the control signals in the second and third controllers contained chattering due to the discontinuous functional sign of the control law, well based on Figs. 4 (d) and 6 (d). It is noticed that the actual response followed the desired path with a very small error. Since the quadrotor can change its morphology every 12 sec, Fig. 8 shows the outputs of the servo motors for the angles required for each proposed shape, with small errors during the change due to the rotation of the arms because switching between different configurations causes significant coupling. The above results showed the efficiency of the proposed control unit in ensuring continuity of control when switching among different configurations during turbulence with trajectory tracking even during switching. These results also showed satisfactory performance and high accuracy in tracking the path.

7.CONCLUSION

This paper investigated the trajectory tracing of a foldable quadrotor under the influence of particular external disturbances. The mathematical model of the foldable quadrotor was presented. A robust control strategy was proposed and applied to a model of the foldable quadrotor, as the proposed control law was effective and nonlinear based on the sliding surface, where the Sliding Mode controller ensured stability and rejected the effect of disturbances. It was observed that the proposed controller ensured that it followed the proposed trajectory with only slight deviations from the trajectory at the beginning and end of the perturbation, with an overshoot of no more than (7.468×10^{-3}) of the x-axis. The y-axis showed minor oscillations lasting 5sec from the start of the disturbance. The altitude showed a good trajectory with an overshoot of (8.069×10^{-2}) at the beginning of the disturbance and an undershoot of (6.725×10^{-2}) at the end of the disturbance. So, it can be concluded that the proposed control unit can maintain the stability of the quadrotor with the rotating arms in the presence of specific external disturbances with a relatively high accuracy of 98% compared to Refs. [11, 22]. However, this quadrotor cannot withstand wind turbulence of more than 1m/sec. In the future, the proposed controller will be developed to remove chatter and achieve better disturbance rejection by designing the observer controller for disturbance estimation.

NOMENCLATURE

b	Thrust coefficient, $N/rad.sec$
d	Drag coefficient, $N/rad.sec$
e	The closed loop error signal, m
g	Gravitational constant, m/sec^2
J_r	Rotor inertia, $\frac{N.m.sec^2}{rad}$
$J_{(xx,yy,zz)}$	Inertia element, $Kg.m^2$
$k_{a(x,y,z)}$	Aerodynamic friction coefficient, $N/m/sec$
$k_{d(x,y,z)}$	Translation drag coefficient, $N/m/sec$
k_i	Proposed SMC tunning parameters
L	length of arm, cm
Greek symbols	
α	Proposed NLPID tunning parameters
β	Proposed NLPID tunning parameters
μ	Proposed NLPID tunning parameters
ε	error, m
φ, θ, ψ	Angular position element, rad
Ω_r	Total rotor speed, deg/sec

REFERENCES

[1] Chen T, Shan J, Liu HHT. **Transportation of Payload Using Multiple Quadrotors via Rigid Connection**. *International Journal of Aerospace Engineering* 2022; **2022**: 2486561.

[2] Kadhim MQ, Hassan MY. **Design and Optimization of Backstepping Controller Applied to Autonomous Quadrotor**. *IOP Conference Series: Materials Science and Engineering* 2020; **881**(1):012128.

[3] Muhsen A, Raafat S. **Optimized PID Control of Quadrotor System Using Extremum Seeking Algorithm**. *Engineering and Technology Journal* 2021; **39**(6):996-1010.

[4] Taha MY, Mohamed MJ, Ucan ON. **Optimal 3D Path Planning for the Delivery Quadcopters Operating in a City Airspace**. *4th International Symposium on Multidisciplinary Studies and Innovative Technologies (ISMSIT)* 2020:1-6.

[5] Alawsi AAA, Jasim BH, Raafat SM. **Improved Positioning of Delivery Quadcopter Using GPS-Accelerometer Multimode Controller and Unscented Kalman Filter**. *IOP Conference Series: Materials*

Science and Engineering 2020; **745**(1): 012018.

[6] Derrouaoui SH, Bouzid Y, Guiatni M, Dib I, Moudjari N. **Design and Modeling of Unconventional Quadrotors**. *28th Mediterranean Conference on Control and Automation (MED)* 2020:721-726.

[7] Zhao N, Luo Y, Deng H, Shen Y. **The Deformable Quadrotor: Design, Kinematics and Dynamics Characterization, and Flight Performance Validation**. *IEEE/RSJ International Conference on Intelligent Robots and Systems (IROS)* 2017:2391-2396.

[8] Dilaveroğlu L, Onurözcan OO. **MiniCoRe: A Miniature, Foldable, Collision Resilient Quadcopter**. *3rd IEEE International Conference on Soft Robotics (RoboSoft)* 2020:176-181.

[9] Kim SJ, Lee DY, Jung GP, Cho KJ. **An Origami-Inspired, Self-Locking Robotic Arm That Can Be Folded Flat**. *Science Robotics* 2018; **3**(17): eaar2915.

[10] Desbiez A, Expert F, Boyron M, Diperi J, Viollet S, Ruffier F. **X-Morf: A Crash-Separable Quadrotor that Morfs Its X-Geometry in Flight**. 7th Workshop on Research, Education and Development of Unmanned Aerial Systems (RED-UAS): 2017:222-227.

[11] Falanga D, Kleber K, Mintchev S, Floreano D, Scaramuzza D. **The Foldable Drone: A Morphing Quadrotor that Can Squeeze and Fly**. *IEEE Robotics and Automation Letters* 2019; **4**(2):209-216.

[12] Derrouaoui SH, Bouzid Y, Guiatni M, Kada H, Dib I, Moudjari N. **Backstepping Controller Applied to a Foldable Quadrotor for 3D Trajectory Tracking**. *17th International Conference on Informatics in Control, Automation and Robotics (ICINCO)* 2020:537-544.

[13] Alexis K, Nikolakopoulos G, Tzes A. **Experimental Model Predictive Attitude Tracking Control of a Quadrotor Helicopter Subject to Wind-Gusts**. *18th Mediterranean Conference on Control & Automation* 2010:1461-1466.

[14] Cabecinhas D, Cunha R, Silvestre C. **Experimental Validation of a Globally Stabilizing Feedback Controller for a Quadrotor Aircraft with Wind Disturbance Rejection**. *2013 American Control Conference (ACC)* 2013:1024-1029.

[15] Ding L, Wang Z. **A Robust Control for an Aerial Robot Quadrotor under Wind Gusts**. *Journal of Robotics* 2018; **2018**:5607362.

[16] Kuantama E, Vesselenyi T, Dzitac S, Tarca R. **PID and Fuzzy-PID Control Model for Quadcopter Attitude with Disturbance Parameter**. *International Journal of Computers Communications & Control* 2017; **12**(4):519-532.

[17] Allison S, Bai H, Jayaraman B. **Modeling Trajectory Performance of Quadrotors under Wind Disturbances**. *AIAA Information Systems-AIAA Infotech at Aerospace* 2018:1-10.

[18] Sierra JE, Santos M. **Wind and Payload Disturbance Rejection Control Based on Adaptive Neural Estimators: Application on Quadrotors**. *Complexity* 2019; **2019**: 6460156.

[19] Almakhles DJ. **Robust Backstepping Sliding Mode Control for a Quadrotor Trajectory Tracking Application**. *IEEE Access* 2020; **8**:5515-5525.

[20] Abro GEM, Asirvadam VS, Zulkifli SABM, Sattar A, Kumar D, Anwer A. **Effects of Unmodelled Dynamic Factors on an Under-Actuated Quadrotor: A Review of Hybrid Observer Design Methods**. *Measurement and Control* 2020; **53**(9-10):1978-1987.

[21] Mustafa Abro GE, Ali ZA, Zulkifli SA, Asirvadam VS. **Performance Evaluation of Different Control Methods for an Underactuated Quadrotor Unmanned Aerial Vehicle (QUAV) with Position Estimator and Disturbance Observer**. *Mathematical Problems in Engineering* 2021; **2021**:8791620.

[22] Meradi D, Benselama ZA, Hedjar R. **A Predictive Sliding Mode Control for Quadrotor's Tracking Trajectory Subject to Wind Gusts and Uncertainties**. *International Journal of Electrical and Computer Engineering* 2022; **12**(5):4861-4875.

[23] Zapar WM, Gaeid K, Mokhlis HB, Al Smadi TA. **Review of the Most Recent Articles in Fault Tolerant Control of Power Plants 2018-2022**. *Tikrit Journal of Engineering Sciences* 2023; **30**(2):103-113.

[24] Khalil MR, Mahmood SB. **Proportional-Integral-Derivative Controller Using Embedded System Design Techniques**. *Tikrit Journal of Engineering Sciences* 2013; **21**(2):44-51.

[25] Derrouaoui SH, Bouzid Y, Guiatni M. **Towards a New Design with Generic Modeling and Adaptive Control of a Transformable Quadrotor**. *Aeronautical Journal* 2021; **125**(1294):2169-2199.

[26] Derrouaoui SH, Bouzid Y, Guiatni M. **PSO Based Optimal Gain Scheduling Backstepping Flight Controller Design for a Transformable Quadrotor**. *Journal of Intelligent and Robotic Systems* 2021; **102**(3):1-21.

[27] Wissal T. **Numerical Model Development of a Transformable Quadrotor**. PhD Dissertation. University of Science and Technology; 2021.

[28] Idrissi M, Annaz F. **Dynamic Modelling and Analysis of a Quadrotor Based on Selected Physical Parameters**. *International Journal of Mechanical Engineering and Robotics Research* 2020; **9**(6):784-790.

[29] Hamoudi AK. **Sliding Mode Controller for Nonlinear System Based on Genetic Algorithm**. *Engineering and Technology Journal* 2014; **32**(11):2745-2759.

[30] Sa WK, Al-Samarraie SA, Kassim AB. **Nonlinear Controller Design for a Mobile Manipulator Trajectory Tracking**. *International Journal of Computer and Communication Engineering* 2014; **14**(3):30-42.

[31] Fitiavana Z, Tongalafatra A, Elisée R, Fils HE. **Modeling the Effects of External Disturbances on a Quadrotor Mini-UAV**. *International Journal of Advanced Research and Innovative Ideas in Education* 2019; **5**(4):573-581.